Always On Air: Adaptive Physical Layer Switching For Uninterrupted UAV Air-to-Ground Communication

Vincenz Mechler
Secure Mobile Networking Lab
TU Darmstadt, Germany
vmechler@seemoo.tu-darmstadt.de

Felix Wiegand
Secure Mobile Networking Lab
TU Darmstadt, Germany
fwiegand@seemoo.tu-darmstadt.de

Matthias Hollick
Secure Mobile Networking Lab
TU Darmstadt, Germany
mhollick@seemoo.tu-darmstadt.de

Bastian Bloessl
Secure Mobile Networking Lab
TU Darmstadt, Germany
mail@bastibl.net

ABSTRACT

Reliable wireless communication is crucial for remote operation of Unmanned Aerial Vehicles (UAVs). Yet, staying in control of the vehicle at all times poses a great challenge, given the dynamics of the wireless channel. Existing technologies are optimized for a given application and, therefore, not well suited for this use case, as they cannot provide both high throughput in high Signal to Noise Ratio (SNR) regimes and high reliability in low SNR regimes. To overcome this limitation, we propose a channel-aware predictive physical layer switching algorithm, utilizing the UAV's telemetry data for implicit synchronization. We evaluate our system experimentally in a fully emulated testbed, achieving an overall outage probability as low as 0.7 % while increasing the average throughput.

CCS CONCEPTS

• **Networks** → **Network experimentation**; **Mobile networks**.

KEYWORDS

Hardware-in-the-loop testbed, link adaptation, software-defined radio

ACM Reference Format:
Vincenz Mechler, Felix Wiegand, Matthias Hollick, and Bastian Bloessl. 2024. Always On Air: Adaptive Physical Layer Switching For Uninterrupted UAV Air-to-Ground Communication. In *The 10th Workshop on Micro Aerial Vehicle Networks, Systems, and Applications (DroNet' 24), June 3–7, 2024, Minato-ku, Tokyo, Japan.* ACM, New York, NY, USA, 6 pages. https://doi.org/10.1145/3661810.3663467

1 INTRODUCTION

The high dynamics and diverse environments in which Unmanned Aerial Vehicles (UAVs) are operated pose a great challenge on the wireless communication link. Existing wireless technologies are optimized for very specific use cases (like broadband Internet access or Low-Power Wide-Area Networks (LPWANs)) and, therefore, not well suited for the remote operation of UAVs. Moving quickly from near-perfect reception with Line-of-Sight (LOS) channels to multi-path channels with low Signal to Noise Ratio (SNR), the communication link to the UAV exceeds the operating range of any single wireless technology. Relying on Wireless LAN (WLAN), for example, provides the required bandwidth for live video streams but will also experience more frequent outages, compared to LPWANs.

This can be problematic, considering that telemetry data and control commands are critical for UAV operation and must not experience prolonged interruptions. Application data like sensor readings or live video streams, in turn, are less critical but usually generate orders of magnitude more traffic, impossible to transmit over an LPWAN link.

To provide the best possible connectivity in all situations, we propose a novel channel-prediction-based Physical Layer (PHY) switching algorithm for the UAV Air-to-Ground (AG) channel and evaluate its performance in a Hardware-in-the-Loop (HITL) testbed. We exploit knowledge of the environment as well as the UAV's dynamics to accurately predict the channel conditions and proactively adapt to minimize outage durations. Thus, we enable the operator to stay in control of the UAV at all times, even in challenging environments with frequent LOS interruptions, while still allowing high throughput secondary transmissions whenever possible.

For synchronization between sender and receiver, only knowledge of the UAV's position is necessary as we use a deterministic and locally stable channel predictor. The position is already part of the critical telemetry data, which our system transmits reliably. Hence, this information is constantly available at both the UAV and the Ground Control Station (GCS). This enables simultaneous switching at both endpoints, preventing additional synchronization overhead. Synchronized switching without prior explicit communication or a timeout mechanism, in turn, reduces downtime in case the receiver cannot listen to all PHYs at the same time, improving the response time of our switching system. Existing systems are either agnostic of the environment, not proactive, or require explicit synchronization, thus, making suboptimal switching decisions and causing longer outage durations and lower average throughput.

Our switching algorithm, furthermore, supports arbitrary PHYs with discrete modes of operation. In this paper, we evaluate the system on a fully emulated testbed for UAV communications using IEEE 802.11g WLAN with different Modulation and Coding Schemes

DroNet' 24, June 3–7, 2024, Minato-ku, Tokyo, Japan

ACM ISBN 979-8-4007-0656-1/24/06…$15.00
https://doi.org/10.1145/3661810.3663467

(MCSs) and the LoRa PHY. The practical evaluations demonstrate the low outage probability and high throughput of our system.

The remainder of this work is structured as follows: In Section 2, we provide background on PHY adaptation and discuss related work. We then detail the design of our PHY switching algorithm, as well as our HITL testbed, in Section 3. Section 4 presents the performance of our proactive algorithm together with the static PHYs and the reactive algorithm as baselines. We discuss limitations of our approach and possible future work in Section 5. Section 6 concludes this paper.

2 BACKGROUND AND RELATED WORK

The possibility to adapt communication protocols as the environment changes is an active field of research. In this work, we focus on the PHY, as it defines limits on achievable throughput, outage probability, and communication range by which the higher layers are bound. We distinguish between PHY adaptation, where a single PHY is used with different parameters and PHY switching, where a communication link utilizes different technologies.

2.1 Physical Layer Adaptation

To a certain degree, PHY adaptation is already part of most modern wireless standards. IEEE 802.11, for example, defines multiple MCSs and an interface for rate adaptation algorithms, i.e., for selecting PHY parameters that best fit the current channel conditions. The actual algorithm is not part of the standard but was the subject of many research studies [2].

However, such standards are usually optimized to narrow use cases and fail to satisfy the demands of the UAV AG link, i.e., high reliability in dynamic environments but also high throughput whenever possible. Combining different standards in an adaptive system can, however, effectively mitigate the weaknesses of any single PHY [5, 6, 8, 10].

Although the line between PHY adaptation and switching can be blurred, we consider a system to be single-PHY, if it uses the same (family of) modulation, error correction and interference avoidance schemes and stays in the same frequency band.

2.2 Soft-Switched Systems

In soft-switched systems, all PHYs can be used simultaneously. Zhang et al. [10] employ Raptor coding to jointly transmit on a Free-Space Optical (FSO) and an RF link. The system reportedly achieves significantly improved throughput over a hard-switched system under identical conditions. This, however, comes at the cost of increased energy consumption and transceiver complexity and necessitates implementation on Field-Programmable Gate Array (FPGA) to keep up with the high data rates.

2.3 Hard-Switched Systems

Systems that use only one PHY at a time can have simpler transceiver structure and lower energy consumption. The possibility to use a single frontend for all PHYs makes these systems well suited for deployment on UAVs, which are usually limited by constraints with regard to size, weight, and power consumption.

This, however, limits the possibilities of synchronizing sender and receiver. For explicit synchronization, a reliable and always available feedback link is required [3]. Usman et al. [8] propose a reactive hybrid FSO/RF system based on receive SNR thresholding. Both links are subject to fading channels. The system is evaluated analytically but uses the ground-truth SNR while assuming perfect synchronization between the endpoints. Our baseline model shows that an SNR-based system without explicit synchronization is not practical, as it incurs frequent interruptions when sender and receiver are out of sync.

Pai and Sainath [6] propose a more complex UAV-assisted relaying system with three PHYs per UAV and multiple UAVs to select from. While the propagation channels are modeled explicitly in the evaluation, the switching overhead is ignored. This leads to the conclusion that the best policy is to always select the PHY with the highest instantaneous SNR, which would potentially result in a high frequency of switching operations and impact the performance of a real system. Since we perform our evaluation experimentally by transmitting signals on the PHY, we inherently include the switching overhead.

Nock et al. [5] also propose a proactive switching algorithm, although based on prediction of the receive SNR from its immediate history, as opposed to prediction from a deterministic channel model. While the system shows significant improvement over reactive SNR-based switching, the issue of synchronization between sender and receiver is not addressed, and the evaluation assumes static throughput for the reliable fallback PHY. The switching decision is communicated out-of-band to both endpoints, so the system cannot be directly deployed to realistic scenarios.

We apply a realistic channel model to all PHYs, including the reliable low-throughput LoRa PHY. In our experiments, the endpoints can only communicate over the uncertain channel and have no outside sources of synchronization. Therefore, our evaluation addresses synchronization, switching overhead, and propagation effects on all PHYs.

3 DESIGN

In this section, we describe our PHY switching algorithm and the HITL testbed that we use to evaluate it in a realistic environment.

3.1 Assumptions

Our algorithm is designed for the UAV AG link between a UAV that is aware of its location and a stationary GCS. For the PHYs, we pre-select several configurations with different range–throughput trade-offs. For the evaluations in this paper, we use IEEE 802.11g with BPSK and 16-QAM modulations (each with coding rate ½ and 20 MHz bandwidth) as well as LoRa with spreading factor 7 and a bandwidth of 500 kHz. Please note that the proposed algorithm is not tied to these PHYs. They are exemplary and were selected because of their different characteristics and the availability of Software Defined Radio (SDR) implementations. Both the UAV and GCS use a single RF frontend and can, therefore, only send and receive on one frequency at a time. If the devices are equipped with multiple frontends for increased robustness through frequency diversity, the same algorithm could be employed on each link.

The UAV sends its own location periodically, together with other telemetry data, like altitude, speed, and heading, while the GCS may send control commands to the UAV. Apart from telemetry data,

the UAV can also transmit a stream of loss-tolerant application data, e.g., live video or sensor data.

The primary goal of our algorithm is to ensure reliable delivery of the telemetry data to stay in control of the vehicle and to avoid triggering failsafe mechanisms of its flight controller. As a secondary objective, we want to transmit as much application data as possible.

3.2 Physical Layer Switching Algorithm

Our algorithm exploits the known or extrapolated position of both endpoints and the relatively predictable UAV AG channel to select the optimal PHY configuration. The UAV knows its own location and that of the fixed GCS, while the GCS knows its own location and receives periodic updates from the UAV, as long as the communication link is operational. With this information, both endpoints can compute the expected attenuation using a deterministic channel model specifically developed for the UAV AG channel. This allows us to calculate the expected SNR, which we use to select the ideal PHY configuration. Since our system maintains the connection and prevents outages of the telemetry data, the position estimate at the GCS is continually updated, and both endpoints stay synchronized.

In order to avoid oscillation near the switching points, we apply a hysteresis of 0.1 dB around the thresholds. This value was determined empirically and might have to be adjusted based on the maximum velocity and acceleration of the UAV.

3.2.1 Channel Prediction. For predicting the channel conditions based on the location of the UAV and the GCS, we use the Curved-Earth Two-Ray (CE2R) model, extended by a model for building shadowing, which attenuates the signal relative to the intersected distance and carrier frequency.

The CE2R model, which was developed specifically for the communication channel between a ground station with an antenna near ground level and an elevated terminal with LOS, such as a UAV, models two distinct propagation paths: the direct LOS ray with attenuation based on Free-Space Path Loss (FSPL) and a ground reflection on the earth's surface, taking into account additional parameters like surface roughness. As each path has a given delay, attenuation, and phase shift, the model can be regarded as a frequency-selective, Tapped Delay Line (TDL) channel model. However, for switching decisions based on a threshold, a single scalar value is desirable. Therefore, we predict the expected attenuation at the current UAV position by combining both rays at the carrier frequency.

To model shadowing by buildings, as is common in urban areas, even with the UAV flying at relatively high altitudes, we rely on OpenStreetMap data.[1] For each building, we get a polygon of its outer shape and its height. Based on this, we compute the intersections of the LOS ray and the ground reflection with any building and apply an attenuation based on the length of the intersection. This approach is inspired by similar channel models used in vehicular networking simulation [7].

3.2.2 UAV Position Extrapolation. We assume that the UAV always knows its location from its GPS receiver. However, the update rates of typical GPS receivers of 1–5 Hz are rather low [9] – much lower than the 100 Hz used by our algorithm. In every cycle, we, therefore, extrapolate the position based on the past trajectory. For this purpose, we employ Kalman filters at the UAV and GCS, updated with the raw GPS measurements and the transmitted telemetry updates, respectively. This way, the GCS can use fine-grained UAV position estimates to drive the channel prediction. Additionally, the GCS can bridge short outages of the telemetry data by extrapolating the UAV position estimate, potentially across the delayed threshold that triggers the switch to a more robust PHY.

While we assume the GCS to be stationary in our implementation, the system could be extended to support mobile GCSs without major modifications. For this, it would be sufficient to also transmit GCS telemetry data to the UAV and to repeat the position estimation procedure for the GCS position.

[1] https://www.openstreetmap.org/

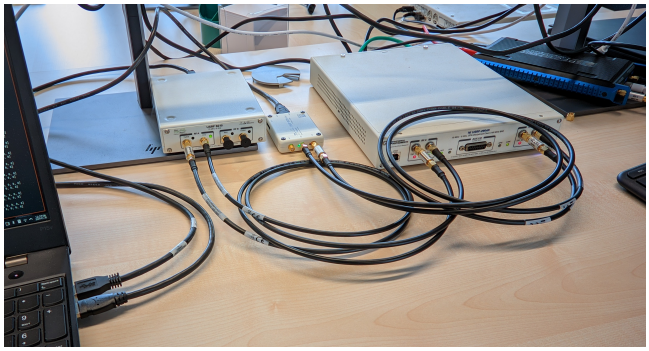

Figure 1: Wireless-in-the-loop testbed setup with SDRs for GCS, UAV, and the channel emulator (left to right).

3.2.3 Threshold Computation. To determine the SNR thresholds, we perform simulated calibration flights for each PHY configuration. To this end, we fly in a straight line away from the GCS and monitor the throughput, expected attenuation, and SNR at the receiver. Using these results, we select the intersection points of the throughput curves for the thresholds.

This calibration has to be done once, and only needs to be repeated when changing the setup, the channel estimator, or the PHY configurations. The physical setup, e.g., the RF frontends, antennas, and gains, directly affect the range of all PHY configurations. Changing the configurations themselves might also result in changed receiver sensitivity. The channel estimator predicts the attenuation caused by the channel but excludes static frontend gains. Thus, the thresholds on the predicted attenuation need to be matched to the actual properties of the setup. Modifying the channel predictor itself would naturally also invalidate previously calibrated thresholds.

3.3 SDR Testbed

To conduct these calibration measurements and evaluate our PHY switching algorithm, we extend our HITL testbed for UAV AG communications [1]. The testbed emulates both the wireless link as well as the flight controller and mission control software on the endpoints. Figure 1 shows an overview of our setup.

3.3.1 UAV and Ground Station. The UAV uses the ArduPilot[2] flight controller that runs in a physical world simulation and communicates with the GCS via MAVLink. GCS control software like QGroundControl[3] is optional in this configuration and can be used for interactive experiments. In addition to the MAVLink messages, we generate best-effort application data for the up- and downlink.

3.3.2 Adaptive Transceiver Design. The adaptive transceiver is implemented using the FutureSDR[4] framework. It includes PHYs for IEEE 802.11g and LoRa, which we run in parallel on both endpoints. The SDRs are connected with either PHY, which can be switched during runtime through FutureSDR's integrated remote control interface. On the UAV, we use a USRP B200mini SDR, which is suitable for mounting on a UAV, while on the GCS, we use a USRP B210 SDR. The devices operate in frequency division duplex, using different carrier frequencies for up- and downlink to exclude effects from channel access schemes, since medium access is out of scope for this paper.

3.3.3 Channel Emulator. Both SDRs are connected via cable to a USRP X310 SDR, which acts as an FPGA-based, bidirectional, wideband (160 MHz) channel emulator [1]. It implements a TDL channel model through a Finite Impulse Response (FIR) filter with up to 41 taps that can be configured live while the system is running, allowing us to model frequency selective fading, attenuation, and Intersymbol Interference (ISI). The taps for the channel emulator are computed with a probabilistic channel model that is based on the deterministic model described earlier but extended with additional intermittent propagation paths, similar to Matolak and Sun [4].

4 EVALUATION

In this section, we present the evaluation results, comparing our PHY switching algorithm to static PHYs (as a baseline) and a reactive switching algorithm. This reactive algorithm does not predict the channel but reacts to SNR changes of received frames. Further, in order to achieve stable switching behavior without synchronization, the UAV always dictates the switches, and the GCS follows after noticing the absence of messages on the previously active PHY.

For the baseline experiments, we consider the three PHY configurations used in our algorithm, i.e., IEEE 802.11g with BPSK and 16-QAM modulations, as well as LoRa with spreading factor 7 and a bandwidth of 500 kHz. The reactive algorithm estimates the received SNR for each frame, averaging over a 700 ms sliding window and uses this value to select the PHY configuration.

4.1 Baseline

To evaluate the system under realistic conditions, we conduct virtual test flights using the Software-in-the-Loop (SITL) flight controller and track the received data while the mission progresses. Figure 2 shows the throughput of the static PHYs over time for a flight plan, where the UAV flies away from the GCS on a straight line, turns, and flies back. Due to the ground reflection, the distance does not directly correlate with attenuation, as the UAV passes through a region with strong destructive interference from the reflected path. As expected, the achievable throughput of IEEE 802.11g is several orders of magnitude higher than LoRa, but it also has a much more limited range. Similarly, 16-QAM provides higher throughput than BPSK but only within approximately 100 m. During the mission, both IEEE 802.11g configurations experience outages, while LoRa provides permanent connectivity, although some frame loss occurs, especially in shadowed regions. Based on these results, we configure the SNR thresholds for both PHY switching strategies (i.e., our proactive algorithm and the reactive strategy).

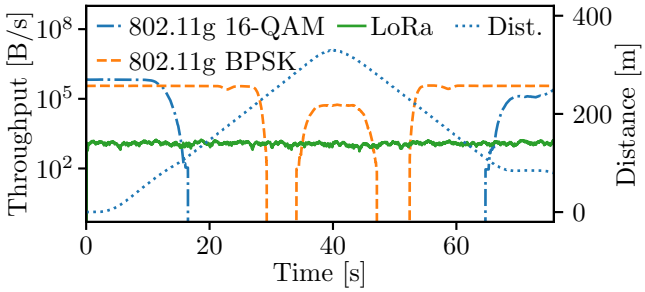

Figure 2: Baseline results, showing the throughput of the three static PHY configurations for the LOS scenario (cf. Figure 3a). Throughput on the left, ground distance between UAV and GCS on the right axis.

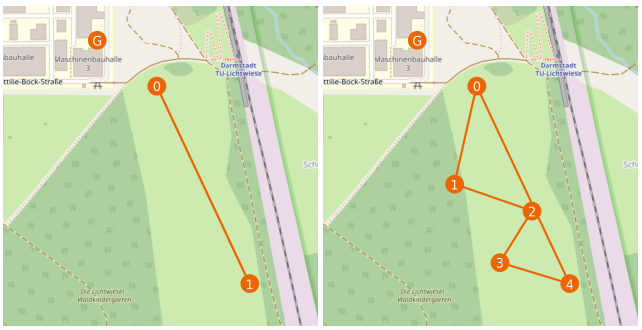

(a) LOS scenario. **(b) Shadowing scenario.**

Figure 3: Flight plans for two exemplary evaluation scenarios. The UAV starts at the GCS (G), flies the depicted path, and returns to waypoint 0.

Due to the long frames of LoRa, the loss of subsequent frames may create maximum outage durations, i.e., the longest duration between reception of frames within a scenario, of several hundred milliseconds. Since interactive control of the UAV requires low latency for the telemetry data, we define the outage probability with a threshold of 0.25 kByte/s over a 200 ms window. With a median of the maximum outage durations over all scenarios of 326 ms, LoRa achieves an outage probability of 1.3 %.

4.2 Evaluation Scenarios

In addition to the straight LOS flight plan, we also evaluate more complex scenarios with shadowing through buildings. Figure 3

[2]https://ardupilot.org/
[3]http://qgroundcontrol.com/
[4]https://www.futuresdr.org/

Table 1: Average throughput (TP), maximum outage duration (OD), and outage probability (OP) for the LOS and shadowing (NLOS) scenarios from Figure 3 individually and aggregated over all 14 evaluation scenarios.

		QAM	BPSK	LoRa	Reactive	Proactive
TP	LOS	99.5	231.1	1.2	200.6	263.3
(kB/s)	NLOS	117.4	138.2	1.1	86.3	137.3
	Total	68.8	182.6	1.1	141.7	202.0
OD	LOS	48871	5971	220	804	301
(ms)	NLOS	67042	18338	402	1137	362
	Total	54585	36862	643	2489	547
OP	LOS	68.3	15.6	0.1	5.7	0.2
(%)	NLOS	81.3	41.3	1.0	9.4	0.5
	Total	75.6	33.7	1.3	8.5	0.7

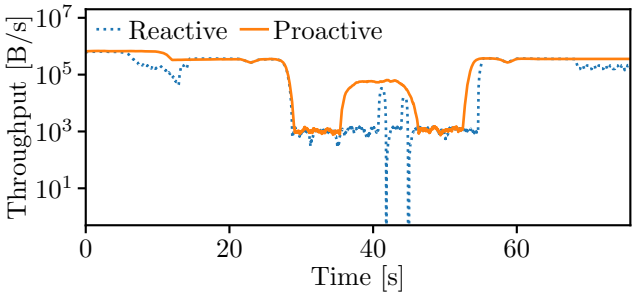

Figure 4: Throughput over mission progress for adaptive PHYs without shadowing during the LOS scenario shown in Figure 3a. Switches to low-throughput PHY caused by entering region with destructive interference. Performance of the static PHYs for the same scenario can be seen in Figure 2.

shows two of our 14 evaluation scenarios. Due to the location of the GCS at the corner of a building, a portion of the area south of the GCS lies within LOS, whereas the remaining part is obscured by the building and, thus, experiences high attenuation.

4.3 Adaptive Physical Layers

In the scenario depicted in Figure 3a, all waypoints lie within LOS of the GCS. The results of this mission are depicted in Figure 4, which shows the throughput for the reactive switching strategy and our proposed proactive algorithm. The reactive switching algorithm can cope with this relatively slowly changing channel, although it is not able to fully exploit the availability of WLAN. Furthermore, the lack of synchronization causes some outages at switching points. Our algorithm, in turn, keeps outage durations at a minimum by proactively switching synchronously at UAV and GCS. Since the GCS never loses downlink connectivity, the UAV position estimate stays synchronized and can be used to predict the next switch.

The scenario shown in Figure 3b is more challenging. Here, the UAV moves in and out of the shadow of a building, which causes sudden changes in the attenuation. The reactive switching algorithm requires some time to differentiate the drop in receive SNR

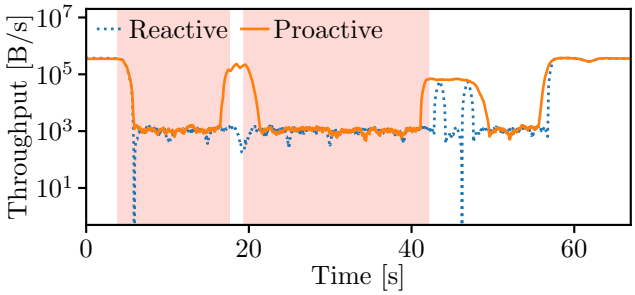

Figure 5: Throughput over mission progress for adaptive PHYs in the presence of strong shadowing. Corresponding mission waypoints illustrated in Figure 3b, shadowed regions shaded in red.

from random fluctuations and initiate a switch. Due to the lack of synchronization, outages from shadowing are, therefore, even more pronounced, as can be seen in Figure 5. Our algorithm, in turn, can deal with abrupt LOS interruptions, as they can be predicted using the channel model. Therefore, our system switches proactively before the connection is interrupted and provides continued connectivity throughout the flight.

Overall, we evaluate 14 scenarios with different flight plans and varying levels of shadowing through buildings. Table 1 summarized the performance of the static PHYs, the reactive baseline, and our proactive algorithm over all scenarios, as well as for the two scenarios shown in Figure 3.

Since the adaptive PHYs use IEEE 802.11g for parts of the scenarios, they are less likely to encounter high outage duration outliers within the shorter sections of LoRa. By also keeping the outages at switching points low, our proactive system can achieve an overall outage probability of 0.7 %. The maximum outage duration per scenario also stays comparable to that of LoRa, with a median of 293 ms and an average of 332 ms. With an overall maximum outage duration of 547 ms over all scenarios, our system ensures constant connectivity and avoids triggering failsafe mechanisms in the flight controller. The reactive algorithm, on the other hand, loses connection for a total maximum of 2.5 s, with an average of 1.31 s and a median of 1.16 s.

In addition, the average throughput increases in comparison to all static PHY configurations. In contrast to the high-throughput PHY, our system bridges the long outage durations, using more robust PHYs; in contrast to the high-reliability PHY, our system can benefit from switching to more performant configurations in high-SNR regimes.

5 DISCUSSION

While our approach shows great performance in our experimental performance evaluation, we also want to discuss potential limitations, as our current scenarios do not consider interference or, in general, larger deviations from our channel model that go beyond the probabilistic component that the channel emulator introduces through the addition of intermittent paths. As a result, we could

experience larger discrepancies between the estimated and the experienced Signal to Noise and Interference Ratio (SNIR), which could lead to outages, requiring fallback mechanisms like timeouts.

To combat this, our approach could be combined with explicit signaling (for example about local interference sources) allowing the endpoints to make more robust predictions. With such a mechanism, it might be possible to localize and map the interference sources during a mission and update the channel model or even feed this information into the flight controller to optimize path planning for wireless connectivity.

Furthermore, our approach relies on accurate positioning at the UAV. While this could be done with LiDAR, radar, or optical systems, it is by far more common to use GPS or any other Global Navigation Satellite System (GNSS). Therefore, a loss of GNSS signals, i.e., by jamming or at low altitudes in dense urban environments, would break the channel prediction mechanism. In this case, we would have to fall back to a reactive approach.

6 CONCLUSIONS

In this paper, we have proposed a proactive, prediction-based PHY switching algorithm for the UAV AG channel. We have shown the benefits of using information about the environment to make an implicitly synchronized switching decision at both endpoints simultaneously. Our system has been evaluated under realistic conditions, using a fully emulated wireless-in-the-loop SDR testbed and an FPGA-based wideband channel emulator. The results have shown that our algorithm achieves consistently lower maximum outage durations than a reactive algorithm. Utilizing high-throughput PHYs whenever possible, our adaptive system can provide substantially higher overall throughput than a static long-range PHY yet retains connectivity throughout challenging environments.

ACKNOWLEDGMENTS

This work has been co-funded by the LOEWE initiative (Hesse, Germany) within the emergenCITY center, as well as the German Research Foundation (DFG) in the Collaborative Research Center (SFB) 1053 MAKI (Project-ID 210487104). The authors acknowledge the financial support by the Federal Ministry of Education and Research of Germany in the project "Open6GHub" (grant number: 16KISK014).

REFERENCES

[1] Lars Baumgärtner, Maximilian Bauer, and Bastian Bloessl. 2023. SUN: A Simulated UAV Network Testbed with Hardware-in-the-Loop SDR Support. In *IEEE Wireless Communications and Networking Conference (WCNC 2023)*. Glasgow, Scotland. https://doi.org/10.1109/WCNC55385.2023.10119014

[2] Saad Biaz and Shaoen Wu. 2008. Rate Adaptation Algorithms for IEEE 802.11 Networks: A Survey and Comparison. In *2008 IEEE Symposium on Computers and Communications (ISCC)*. Marrakech, Morocco. https://doi.org/10.1109/ISCC.2008.4625680

[3] Emrecan Demirors, George Sklivanitis, G. Enrico Santagati, Tommaso Melodia, and Stella N. Batalama. 2018. A High-Rate Software-Defined Underwater Acoustic Modem With Real-Time Adaptation Capabilities. *IEEE Access* 6 (March 2018). https://doi.org/10.1109/ACCESS.2018.2815026

[4] David W. Matolak and Ruoyu Sun. 2017. Air–Ground Channel Characterization for Unmanned Aircraft Systems—Part III: The Suburban and Near-Urban Environments. *IEEE Transactions on Vehicular Technology* 66, 8 (Aug. 2017). https://doi.org/10.1109/TVT.2017.2659651

[5] Kristen Nock, Carlos Font, and Michael Rupar. 2016. Adaptive Transmission Algorithms for a Hard-Switched FSO/RF Link. In *IEEE Military Communications Conference (MILCOM)*. Baltimore, MD. https://doi.org/10.1109/MILCOM.2016.7795440

[6] Vinay U. Pai and B. Sainath. 2021. UAV Selection and Link Switching Policy for Hybrid Tethered UAV-Assisted Communication. *IEEE Communications Letters* 25, 7 (July 2021). https://doi.org/10.1109/LCOMM.2021.3070197

[7] Christoph Sommer, David Eckhoff, Reinhard German, and Falko Dressler. 2011. A Computationally Inexpensive Empirical Model of IEEE 802.11p Radio Shadowing in Urban Environments. In *8th IEEE/IFIP Conference on Wireless On demand Network Systems and Services (WONS 2011)*. Bardonecchia, Italy. https://doi.org/10.1109/WONS.2011.5720204

[8] Muneer Usman, Hong-Chuan Yang, and Mohamed-Slim Alouini. 2014. Practical Switching-Based Hybrid FSO/RF Transmission and Its Performance Analysis. *IEEE Photonics Journal* 6, 5 (Oct. 2014). https://doi.org/10.1109/JPHOT.2014.2352629

[9] Jong-Hwa Yoon and Huei Peng. 2013. A Cost-Effective Sideslip Estimation Method Using Velocity Measurements From Two GPS Receivers. *IEEE Transactions on Vehicular Technology* 63, 6 (Dec. 2013). https://doi.org/10.1109/TVT.2013.2294717

[10] Wenzhe Zhang, Steve Hranilovic, and Ce Shi. 2009. Soft-Switching Hybrid FSO/RF Links Using Short-Length Raptor Codes: Design and Implementation. *IEEE Journal on Selected Areas in Communications* 27, 9 (Dec. 2009). https://doi.org/10.1109/JSAC.2009.091219